AGU PUBLICATIONS

JGR

Journal of Geophysical Research: Biogeosciences

RESEARCH ARTICLE
10.1002/2014JG002874

**Key Points:**
- Deep sediments (>10 cm) are nitrate sinks in groundwater-fed rivers
- Denitrification can be sustained without substantial buried organic matter
- Denitrification in a sand-dominated reach can be transport-controlled

**Supporting Information:**
- Supporting Information S1

**Correspondence to:**
C. M. Heppell,
c.m.heppell@qmul.ac.uk

**Citation:**
Lansdown, K., C. M. Heppell, M. Trimmer, A. Binley, A. L. Heathwaite, P. Byrne, and H. Zhang (2015), The interplay between transport and reaction rates as controls on nitrate attenuation in permeable, streambed sediments, *J. Geophys. Res. Biogeosci.*, *120*, 1093–1109, doi:10.1002/2014JG002874.

Received 4 DEC 2014
Accepted 6 MAY 2015
Accepted article online 14 MAY 2015
Published online 20 JUN 2015



# The interplay between transport and reaction rates as controls on nitrate attenuation in permeable, streambed sediments

**K. Lansdown[1,2], C. M. Heppell[1], M. Trimmer[2], A. Binley[3], A. L. Heathwaite[3], P. Byrne[3,4], and H. Zhang[3]**

[1]School of Geography, Queen Mary, University of London, London, UK, [2]School of Biological and Chemical Sciences, Queen Mary, University of London, London, UK, [3]Lancaster Environment Centre, Lancaster University, Lancaster, UK, [4]Now at School of Natural Sciences and Psychology, Liverpool John Moores University, Liverpool, UK

**Abstract** Anthropogenic nitrogen fixation and subsequent use of this nitrogen as fertilizer have greatly disturbed the global nitrogen cycle. Rivers are recognized hot spots of nitrogen removal in the landscape as interaction between surface water and sediments creates heterogeneous redox environments conducive for nitrogen transformations. Our understanding of riverbed nitrogen dynamics to date comes mainly from shallow sediments or hyporheic exchange flow pathways with comparatively little attention paid to groundwater-fed, gaining reaches. We have used $^{15}N$ techniques to quantify in situ rates of nitrate removal to 1 m depth within a groundwater-fed riverbed where subsurface hydrology ranged from strong upwelling to predominantly horizontal water fluxes. We combine these rates with detailed hydrologic measurements to investigate the interplay between biogeochemical activity and water transport in controlling nitrogen attenuation along upwelling flow pathways. Nitrate attenuation occurred via denitrification rather than dissimilatory nitrate reduction to ammonium or anammox (range = 12 to >17,000 nmol $^{15}N\,L^{-1}\,h^{-1}$). Overall, nitrate removal within the upwelling groundwater was controlled by water flux rather than reaction rate (i.e., Damköhler numbers <1) with the exception of two hot spots of biogeochemical activity. Deep sediments were as important a nitrate sink as shallow sediments with fast rates of denitrification and short water residence time close to the riverbed surface balanced by slower rates of denitrification and water flux at depth. Within this permeable riverbed >80% of nitrate removal occurs within sediments not exposed to hyporheic exchange flows under base flow conditions, illustrating the importance of deep sediments as nitrate sinks in upwelling systems.

## 1. Introduction

The global challenge of nitrate saturation of freshwater environments arises from increased nitrogen loading to rivers due to anthropogenic activities such as land use change, domestic and industrial wastewater treatment, and intensification of agricultural practice [*Bernot and Dodds*, 2005; *Caraco and Cole*, 1999]. In the United Kingdom, nitrate concentrations in many rivers and groundwaters have increased since the 1970s [*Burt et al.*, 2011] leading to coastal eutrophication [*Maier et al.*, 2009], and increasing the costs of drinking water supply in order to meet standards designed to protect the environment [*Knapp*, 2005; *National Audit Office*, 2010]. Monitoring data for regulatory purposes indicate that while nitrate concentrations in many UK rivers have now plateaued, that concentrations in groundwater-fed rivers continue to rise [*Burt et al.*, 2011; *Howden and Burt*, 2008]. This nitrate legacy has renewed interest in the role that naturally occurring microbially mediated processes might play in transforming (e.g., dissimilatory nitrate reduction to ammonium) and removing (in the case of denitrification and anaerobic ammonium oxidation, anammox) nitrate in riverbeds [*Rivett et al.*, 2008; *Stelzer and Bartsch*, 2012].

Considerable attention has been placed on the potential role of the hyporheic zone for nitrate removal from surface waters via denitrification [*Smith*, 2005] and on hyporheic exchange flows (HEFs) as a means of delivering nitrate-rich surface water to the streambed where microbial activity and denitrification rates are enhanced [*Findlay et al.*, 2003; *Fischer et al.*, 2005]. Problems of nitrate enrichment are particularly pertinent, however, for groundwater-fed rivers in permeable catchments with high N-loading rates where nitrate-rich groundwater will dominate base flow. The need to understand nitrogen transformations in gaining river settings have led to an alternative "bottom-up" rather than "top-down" conceptualization of nitrate removal processes, highlighting the importance of measuring nitrogen transformations in deep

stream sediments [*Stelzer and Bartsch*, 2012]. Many experimental studies of nitrogen cycling in streams focus on the upper 10 cm of the riverbed often selecting to conduct experiments ex situ by physically removing sediments, which changes the redox environment and supply of reactants making investigation of the complete nitrogen cycle impossible [*Addy et al.*, 2002; *Sheibley et al.*, 2003]. Likewise, where field studies of nitrogen transformations are attempted, the general approach has been to focus on "soft" riverbed sediments due to the logistical difficulties associated with working within armored gravel or cobble-sized material [*Stelzer and Bartsch*, 2012]. To advance our understanding it is critical that we measure in situ rates of denitrification along with other components of the nitrogen cycle (such as nitrification, anammox, and $N_2O$ production), at depths greater than 10 cm in the coarse-grained sediments typical of groundwater-fed systems, so that the relative importance of denitrification in comparison with other nitrate removal processes can be fully evaluated. Application of $^{15}N$-labeled substrates is the only method by which multiple pathways of nitrogen cycling can be investigated directly and simultaneously. Injection of $^{15}NO_3^-$ into saturated sediments and recovery of porewaters over time (referred to as "push-pull" sampling [*Istok et al.*, 1997]) has been performed at depth within the riverbed and also through groundwater monitoring wells [*Addy et al.*, 2002; *Clilverd et al.*, 2008]. These measurements, however, were focused on quantifying denitrification within large volumes of sediment (10–20 L of tracer were injected) and, consequently, had quite wide vertical resolution (e.g., 30–60 cm). Finer-scale $^{15}N$ push-pull investigations have also been performed [*Burgin and Hamilton*, 2008; *Lansdown et al.*, 2014; *Sanders and Trimmer*, 2006], but to date, not in conjunction with detailed hydrologic measurements.

The extent to which nitrate is exported from groundwater to surface waters in an upwelling groundwater setting will be controlled by the rate of biogeochemical nitrate removal and the flux of water through the riverbed. The Damköhler number, a dimensionless ratio of reaction rate to transport rate of the solute, can be used to contrast the importance of these two drivers of nitrate removal [*Gu et al.*, 2007; *Ocampo et al.*, 2006]. Damköhler numbers have been widely used in contaminant studies in the hydrogeological literature [*Bahr and Rubin*, 1987] and have also been applied to denitrification in hyporheic zones to distinguish between hydrological and biogeochemical controls on nitrate removal from thalweg and marginal sediments [*Harvey et al.*, 2013]. Recent modeling studies have focused on using residence time analysis to distinguish between zones of net nitrification and denitrification along hyporheic flow pathways [*Bardini et al.*, 2012; *Marzadri et al.*, 2011; *Zarnetske et al.*, 2012]. Other processes of nitrate reduction, such as anammox have largely been ignored because their role in nitrate removal is currently thought by many researchers to be negligible [*Burgin and Hamilton*, 2007].

*Stelzer and Bartsch* [2012] have recently developed a conceptual model of nitrate-rich gaining fluvial settings, in which nitrate-rich oxic groundwater upwells through deeper riverbed sediments to reach a zone enriched with electron donors in the form of particulate organic matter from surface waters. This organically enriched layer, arising from the deposition and burial of particulate organic matter and varying in thickness (dependent on deposition rate, vertical hydraulic gradient, and porosity), facilitates the development of hypoxic and anoxic conditions to drive nitrate reduction processes such as denitrification. To date this "bottom-up" conceptualization of gaining reach settings has focused on the interaction of upwelling groundwater with shallow hyporheic exchange flows (HEF). Here we develop the conceptual model further to evaluate the effect of deeper ($>$10 cm depth) horizontal subsurface flows on nitrate reduction processes.

We have previously used measurements of saturated hydraulic conductivity with vertical head gradient from a network of piezometers in a gaining, permeable sandstone reach to show that even in a strongly upwelling stream horizontal water fluxes (both lateral and longitudinal; Figure 1a) can influence of on hyporheic zone chemistry [*Heppell et al.*, 2013]. By combining measurement of water flux with an understanding of the spatial variability in redox patterns in the reach we could distinguish nitrate-rich oxic conditions associated with upwelling groundwater from nitrate-poor reducing conditions associated with horizontal flows from hyporheic exchange and/or riparian flows [*Heppell et al.*, 2013]. We did not observe nitrate-poor, reducing conditions associated with strong groundwater upwelling, probably because the regional aquifer contains little organic carbon [*Smith and Lerner*, 2008] and, as a result, is oxygenated [*Lapworth et al.*, 2008]. Here we combine our 3-D measurements of spatial variability in vertical and horizontal hydrological fluxes (at a spatial resolution not previously captured in gaining stream settings) with in situ process-based measurements of nitrate transformations to investigate the interplay between hydrological and

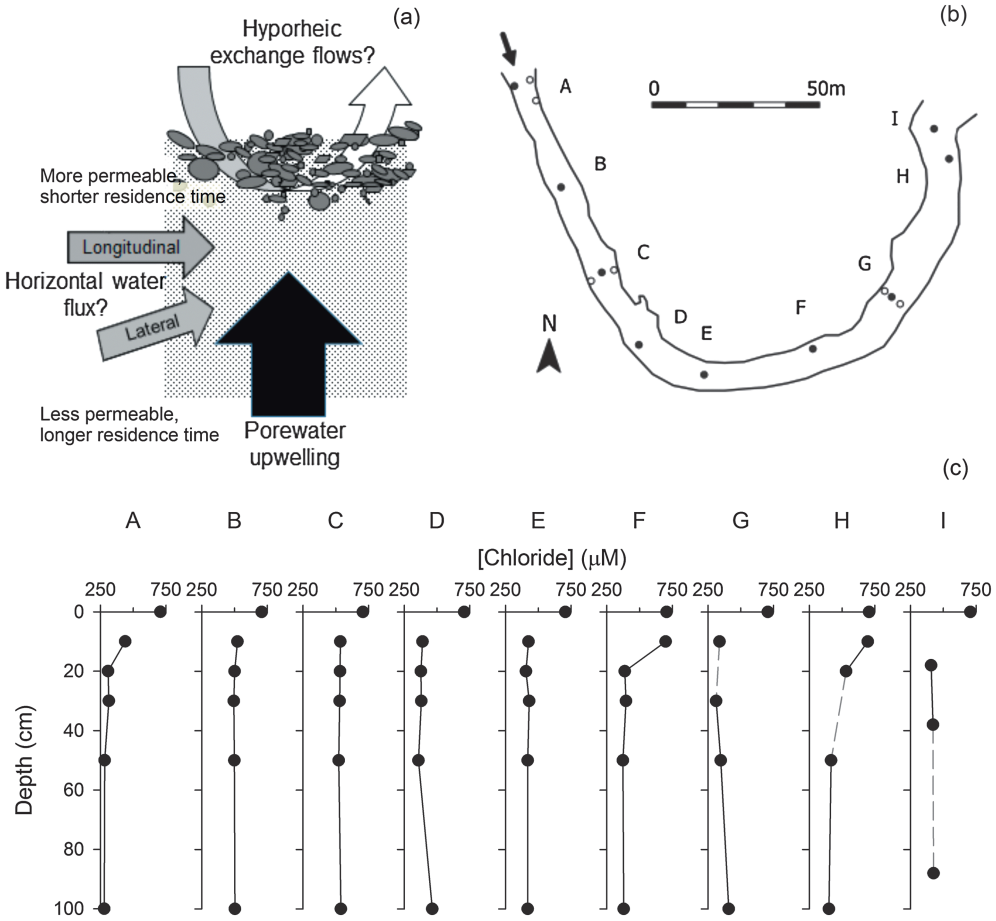


**Figure 1.** (a) Conceptual model of subsurface flow pathways, (b) schematic of the study reach showing piezometers used in $^{15}NO_3^-$ injections, and (c) depth profiles of chloride concentrations along the thalweg of the reach. The black circles indicate piezometers used in thalweg profiles; the white circles are piezometers used for this research but not included in thalweg profiles. Each circle represents a cluster of 3 piezometers (20, 50, and 100 cm).

biogeochemical controls on nitrate consumption at the reach scale. We apply Damköhler numbers in order to distinguish between residence time and biogeochemical controls on nitrate reduction in the stream sediments of our gaining reach.

Specifically, we (1) identify the spatial variability in nitrate consumption in a single gaining reach, focusing on the depth distribution of nitrate attenuation; (2) investigate the factors that controls nitrate consumption in the reach, using Damköhler numbers to explore the interplay between residence time (hydrological) and biogeochemical controls on nitrate consumption; and (3) estimate total nitrate consumption within the riverbed using our in situ hydrological and biogeochemical measurements to quantify the significance of nitrate removal in deep (>10 cm) bed sediments of a gaining reach.

## 2. Methods

### 2.1. Site Description

Our 200 m study site, located within the River Leith (Cumbria, UK), receives groundwater from the Aeolian Penrith Sandstone, a major aquifer of the Permo-Triassic Sandstone in the UK [*Allen et al.*, 1997; *Seymour et al.*, 2008]. The gaining reach comprises sandstone bedrock overlain by unconsolidated glaciofluvial sands and silts (1–2 m), which are topped by sand, gravel, and cobbles forming riffle and pool sequences. The catchment of the River Leith is a mixed agricultural landscape, and the river is a designated Site of Special Scientific Interest and Special Area of Conservation.

### 2.2. Field Sampling Campaign

Riparian and in-stream piezometers (internal diameter = 27 mm) were installed in clusters at the site in June 2009 and June 2010 using a percussion drill (see *Binley et al.* [2013] for a detailed description). Each in-stream cluster comprised three piezometers screened at 100 cm, 50 cm, and 20 cm depth to measure saturated hydraulic conductivity and head gradient. The 100 cm in-stream piezometers were fitted with multilevel porewater samplers at target depths of 10, 20, 30, 50, and 100 cm in order to establish porewater chemistry and to enable tracers to be introduced at various depths beneath the riverbed surface. The end of each porewater sampler was wrapped in a fine polyester mesh to prevent ingress of sediment. Collection of porewater samples (total $n = 72$), $^{15}N$ injections into the multilevel porewater samplers, and measurement of vertical hydraulic gradient was performed at nine points along the study reach (labeled A–I in Figure 1b) from 9 to 13 August 2011 under low flow conditions ($<0.5\ m^3\ s^{-1}$). At positions A, C, and G a transect of three piezometer clusters were examined (total number of piezometer clusters = 15) and we were unable to collect porewater from three sampling tubes (G-20 cm, H-30 cm, and I-50 cm).

#### 2.2.1. Porewater Sampling

Prior to the injection of $^{15}N\text{-}NO_3^-$ (see below), a 40 mL porewater sample was collected from each of the multilevel samplers via a syringe. A sample of surface water was also collected at each piezometer cluster. Samples for analysis of chloride and nitrogen species were filtered (0.2 μm polypropylene membrane, VWR International, UK) into plastic vials (polypropylene) in the field and frozen until later chemical analysis (see below). Samples for analysis of dissolved organic carbon (DOC) were filtered into acid-washed amber glass bottles and acidified to pH < 2 with HCl in the field. For determination of reduced iron (Fe(II)), 1 mL of water was filtered through an oxygen free nitrogen-flushed 0.2 μm filter (as above) into 4 mL of phenanthroline-acetate buffer solution and stored in the dark until analysis by UV-spectrophotometry [*American Public Health Association-American Water Works Association-Water Pollution Control Federation*, 1976; *Grace et al.*, 2010]. Water samples were also collected to determine the natural abundance $^{15}N$ content of nitrogen gas ($N_2$) and dissolved nitrous oxide ($N_2O$) and methane concentrations. Gas tight vials (Exetainer, Labco) were overflowed at least 2 times by gentle discharge of water through a 21-gauge needle to minimize atmospheric exchange, and bacterial activity was inhibited by addition of zinc chloride (25 μL, 7 M). Dissolved oxygen ($O_2$) concentration was measured in the field using a calibrated, fast response electrode (50 μm, Unisense, Denmark). Water temperature and pH were measured (pH-100, VWR International, UK) following $O_2$ determination. For these measurements, water was gently transferred via a three-way stop cock from the collection syringe into an open syringe barrel containing the $O_2$ electrode or pH probe. We determined the amount of $O_2$ contamination that occurred during sample transfer to be approximately 10 μM and corrected all measured $O_2$ concentrations accordingly.

#### 2.2.2. In Situ Measurement of Riverbed Nitrate Reduction

$^{15}N$-labeled $NO_3^-$ tracer (98 atom % $^{15}N$, Sigma Aldrich) solution was prepared in the laboratory at approximately the same concentration as ambient $^{14}NO_3^-$ (100, 200, 300, 400, or 500 μM $^{15}NO_3^-$) and deoxygenated by bubbling with oxygen-free nitrogen gas (British Oxygen Company). The tracer matrix was artificial river water [*Smart and Barko*, 1985] tailored to match the major ion chemistry of the River Leith but with added chloride (~4 mM KCl) to measure advective flow [*Lansdown et al.*, 2014]. In the field, tracer was drawn into luer-lock syringes under oxygen-free nitrogen or after sparging with air to match ambient $O_2$ conditions. Subsamples of the tracer ($n = 3$ per piezometer cluster) were reserved for later chemical analysis and physicochemical measurements (as above and see below). Fifty milliliter of $^{15}N\text{-}NO_3^-$ tracer was injected into the riverbed via each multilevel sampler, with all injections at a piezometer completed within 2.5 h. Porewater samples ($n = 4$, 7 mL) were collected over time after the dead volume of the sampling tube had been discarded. The first porewater sample was recovered immediately after injection. Recovery of porewaters thereafter occurred according to depth with collection of porewater from 10 and 20 cm samplers at 5, 10, and 30 min post injection; 30 and 50 cm samplers at 10, 30, and 60 min post injection and 100 cm samplers at 15, 45, and 120 min post injection. Recovered porewater samples were split between gas-tight vials for $N_2$ analysis and filtered into plastic tubes for anion analysis (using above sampling procedures and analysis methods described below).

We worked from downstream to upstream, and from shallow to deep samplers, to ensure that there was no cross contamination of tracer plumes. Water flux was also sufficiently slow to prevent mixing of tracer injected at different depths within the experimental time frame (see Results). Assuming that the injection

of the tracer forms a sphere centered at the terminus of the multilevel sampler tube, the magnitude of the $^{15}NO_3^-$ dilution immediately post injection corresponds to a sediment volume of 120 $cm^3$ (porosity = 0.35). Accordingly, each of our denitrification measurements has a vertical resolution of approximately ±3.2 cm.

#### 2.2.3. Hydrological and Sediment Analyses

Sediment samples, collected from each core during piezometer installation, were divided into 10 cm increments in the field. On return to the laboratory, the sediment samples were air-dried and divided for loss on ignition (LOI) and granulometric analysis by sieving and laser diffraction. The <1 mm fraction was digested with 30% hydrogen peroxide to remove organic matter, and the samples was dispersed in Calgon before particle size analysis with a Malvern 2000 Mastersizer (Malvern Instruments Ltd., UK). Data from all size distributions were then combined to calculate $d_{50}$ (mm).

Saturated hydraulic conductivity was measured using falling and rising slug tests in the piezometers at 100, 50, and 20 cm depth (see *Binley et al.* [2013] for detailed description). Head levels in the in-stream and bank piezometers were measured concurrently with push-pull measurements using an electronic dipmeter. Darcian vertical water flux ($m\,d^{-1}$) at 100, 50, and 20 cm depth was calculated following the method described in *Binley et al.* [2013], assuming permeability is isotropic.

### 2.3. Laboratory Analyses

#### 2.3.1. Porewater Analysis

Nitrate (limit of detection (LOD) 12 μM, precision 3%) and chloride (LOD 2 μM, precision 1%) were determined using ion exchange chromatography (Dionex ICS2500) while ammonium and nitrite were determined by automated colorimetric analysis (Skalar San++) with detection limits and precision of 0.3 μM ± 5% and 0.05 μM ± 1%, respectively. DOC was analyzed by the nonpurgeable organic carbon method (Thermo TOC analyzer; LOD 23 μM, precision 5%). $N_2O$ and methane were determined using gas chromatography (Agilent Technologies) with electron capture and flame ionization detection, respectively, following addition of a helium headspace (see below).

#### 2.3.2. Calculating In Situ Rates of Nitrate Reduction

A 500 μL helium headspace was introduced to each 3 mL gas-tight vial and equilibrated with the porewater overnight at 22°C. The $^{15}N$-$N_2$ content was quantified using mass-to-charge ratios of 28, 29, and 30 measured with a mass spectrometer (Finnigan MAT DeltaPlus) calibrated and corrected for drift following the procedure described in *Trimmer et al.* [2006]. Precision as a coefficient of variation was better than 1%. Production of $^{29}N_2$ or $^{30}N_2$ was quantified as excess above natural abundance, adapted from *Thamdrup and Dalsgaard* [2000]:

$$\Delta N_{2\ t=i}(\mathrm{nM\ N_2}) = \left[\left(\frac{^{x}N_2}{\Sigma N_2}\right)_{t=i} - \left(\frac{^{x}N_2}{\Sigma N_2}\right)_{\mathrm{background}}\right] \times \Sigma N_2\,\mathrm{sample} \times \alpha^{-1} \times V_s^{-1} \quad (1)$$

where $\Delta^xN_2$ is the amount of excess $^{29}N_2$ or $^{30}N_2$ in the recovered porewater at time = $i$, $^xN_2/\Sigma N_2$ represents the ratio of the $^{29}N_2$ or $^{30}N_2$ mass spectrometer signal to the total $N_2$ signal ($\Sigma N_2 = {}^{28}N_2 + {}^{29}N_2 + {}^{30}N_2$) for either time series or background samples, $\alpha$ is the calibration factor (signal: nmol $N_2$ $vial^{-1}$), and $V_s$ is the volume of porewater in the gas-tight vial (L $vial^{-1}$). "Excess" concentrations of $^{29}N_2$ and $^{30}N_2$ in the tracer solution were also calculated via equation (1) (where $t = i$ is the tracer) to allow correction for loss through advective flow as follows:

$$\Delta'^{x}N_{2\ t=i}(\mathrm{nM\ N_2}) = \Delta^xN_{2\ t=i} + \left[\left(\frac{[Cl^-]_{t=i} - [Cl^-]_{\mathrm{tracer}}}{[Cl^-]_{\mathrm{background}} - [Cl^-]_{\mathrm{tracer}}}\right)\right] \times \Delta^xN_{2\ \mathrm{tracer}} \quad (2)$$

where: $\Delta'\,^xN_2$ is the concentration of $^{29}N_2$ or $^{30}N_2$ at time = $i$ corrected for the loss of $^{15}NO_3^-$ tracer or $^{15}N$ labeled products via advective flow; $\Delta\,^xN_{2\ t=i}$ and $\Delta\,^xN_2$ tracer are the excess of concentration of $^{29}N_2$ or $^{30}N_2$ calculated from equation (1) in the time series samples and tracer solution, respectively, and $[Cl^-]$ is the concentration of chloride in the tracer solution (tracer), ambient porewater (background), and porewater collected over time following the injection of $^{15}NO_3^-$ ($t = i$).

The rate of $^{29}N_2$ and $^{30}N_2$ production ($p^{29}N_2$ or $p^{30}N_2$) was calculated by linear regression of $\Delta'\,^xN_2$ $t = i$ against time. The rate of denitrification was calculated according to *Nielsen* [1992]:

$$\mathrm{Denitrification}\ \left(\mathrm{nmol}\,^{15}\mathrm{N\text{-}N_2\,L^{-1}\,h^{-1}}\right) = p^{29}N_2 + 2 \times p^{30}N_2 \quad (3)$$

**Table 1.** Summary of Denitrification Calculations

| Parameter | Method of Calculation |
|---|---|
| Rate-determined proportion[a] | $\frac{\text{Denitrification rate } \left(\text{nmol}^{15}\text{N-N}_2\ \text{L}^{-1}\text{h}^{-1}\right)_{\text{depth=i}}}{\sum \text{Denitrification rate}_{\text{depth=10,20,30,50,100 cm}}}$ |
| Depth-integrated proportion[b] | $\frac{\text{Denitrification rate } \left(\text{nmol}^{15}\text{N-N}_2\ \text{L}^{-1}\text{d}^{-1}\right)_{\text{depth=i}} \times \text{residence time (d)}_{\text{depth=i}\rightarrow\text{i}'}}{\sum \text{Denitrification rate}_{\text{depth=10,20,30,50,100 cm}} \times \text{residence time (d)}_{\text{depth=0-10,-20,20-30,30-50,50-100 cm}}}$ |
| Areal rate[ab] | $\sum \frac{1}{2}\left[\begin{array}{l}\text{Denitrification rate } \left(\mu\text{mol m}^{-3}\text{h}^{-1}\right)_{\text{depth=i}} \times (\text{depth}_{\text{i}} - \text{depth}_{\text{i}'}(\text{m})) \\ +\text{Denit. rate}_{\text{depth=i}'} \times (\text{depth}_{i} - \text{depth}_{i'})\end{array}\right]$ |
| Damköhler number | $\text{Residence time (h)} \div \frac{1}{\frac{\text{Denit. rate } \left(\text{nmol}^{15}\text{N-N}_2\ \text{L}^{-1}\text{h}^{-1}\right)}{K_m\,(\text{nM})}}$ |

[a]Depth = *i* denotes any of the depths sampled (10, 20, 30, 50, and 100 cm).
[b]$i \rightarrow$ i′ is the distance between depth = *i* and that sampled above (*i*′).

Note that as the $^{15}$N-labeling of the $N_2$ and $N_2O$ produced after injection of $^{15}NO_3^-$ was the same (see Results) then the contribution of anammox to the production of $N_2$ gas could be assumed to be negligible [*Trimmer et al.*, 2006] and, as a consequence, Nielsen's original formulation for the isotope pairing technique remained perfectly valid [*Risgaard-Petersen et al.*, 2003].

The $^{15}$N-labeling of the $N_2O$ pool following injection of $^{15}NO_3^-$ was determined on a subset of samples ($n = 49$). To quantify $^{15}$N-$N_2O$ a 100 μL subsample of the headspace of the gas-tight vial (from above) was injected into an air-filled 12 mL gas-tight vial (Exetainer, Labco). The entire content of the gas-tight vial was swept, using a two-way needle and analytical grade helium, to a trace gas preconcentrator (Cryo-Focusing; PreCon, Thermo-Finnigan), where the gases are dried and cryo-focused twice in liquid $N_2$ and before final separation of $N_2O$ from $CO_2$ on a PoraPLOT Q capillary column. The sample then passes to mass spectrometer (as above) and the mass-to-charge ratios of 44, 45, and 46 are measured. The amount of dissolved $^{15}$N-$N_2O$ was calculated by multiplying the total concentration of $N_2O$, as measured by gas chromatography, by the proportion of $^{15}$N-label in the $N_2O$ pool as determined by mass spectrometry (mass-to-charge = 45/2 × mass-to-charge = 46). Concentrations of $^{15}$N-$N_2O$ were corrected for losses due to advective flow as per equation (2), substituting $N_2O$ for $N_2$ values. Rates of $^{15}$N-$N_2O$ production were then calculated by linear regression of the corrected concentrations against time.

### 2.4. Data Analyses

#### 2.4.1. Assigning Piezometer Clusters to Hydrologic Setting Using Porewater Chemistry

Each piezometer cluster was assigned to one of three hydrologic settings using chloride concentrations in a two end-member mixing model as follows:

$$\text{Mixing score} = \frac{[Cl^-]_{\text{porewater}} - [Cl^-]_{\text{surface water}}}{[Cl^-]_{\text{surface water}} - [Cl^-]_{\text{100 cm}}} \quad (4)$$

where "porewater" refers to samples collected between 10 and 50 cm depth in the riverbed and "100 cm" was porewater recovered from 100 cm. Scores can range from −1 to 0. The lower range indicates dominance of upwelling porewater, and the higher range indicates maximum surface water influence. Hydrology at piezometer was classed as strong porewater upwelling when scores were −1 and hyporheic exchange flows (HEF) when scores vary between −1 and 0. Horizontal water fluxes, for example, longitudinal flow along the river channel or lateral inputs from the riparian zone, were inferred when scores were $<-1$ (no scores were $>0$). As such, horizontal water fluxes cannot be detected with this method if chloride concentrations of the horizontal source are the same as surface water and upwelling porewater. We are confident, however, that the assigned hydrologic settings reflect actual subsurface hydrology as classifications compare favorably with the zones of upwelling, HEF and horizontal fluxes inferred through in situ measurements by *Binley et al.* [2013].

#### 2.4.2. Calculations for Integrating Flux and Nitrate Removal in Sediment via Denitrification

Initially, we examined the relative importance of denitrification activity at different depths in the riverbed by simply contrasting rates of reaction, as per [*Stelzer et al.*, 2011, 2012]. The proportion of denitrification activity at each depth was determined by dividing the individual rate by the sum of all rates within a piezometer cluster (Table 1). We refer to these data as rate-determined proportions.

Nitrate removal within a riverbed will depend not only upon the denitrification rate (as above) but also on amount of time a parcel of water is exposed to a given denitrification rate (as per *Harvey et al.* [2013]). In order to explore the effects of spatial variations in upwelling water flux on the extent of nitrate removal via denitrification we calculated the residence time of upwelling water in each sediment section (0–10 cm, 10–20 cm, etc.) where residence time was the inverse of the relevant Darcy vertical water flux. We measured saturated hydraulic conductivity at 20, 50, and 100 cm depths only, so we estimated residence time of the 0–10 cm and 30–50 cm depth bands by assuming vertical flux at 10 cm was equal to vertical flux at 20 cm and the vertical flux at 30 cm was the average of fluxes at 20 and 50 cm. We then multiplied the in situ rate of denitrification (nmol $^{15}N$-$N_2$ $L^{-1}$ $h^{-1}$) by the residence time ($h$) to calculate the amount of nitrate removed from each sediment section as upwelling water passed through it. In order to express this nitrate removal on a sediment volume basis (mmol N $m^{-3}$) we assumed a sediment porosity of 0.35 (−). Relative magnitudes of denitrification activity within each sediment section were calculated as above; however, we refer to these data as depth-integrated proportions.

Areal rates of denitrification (μmol N $m^{-2}$ $h^{-1}$) were estimated by converting measured denitrification rates (per volume of porewater) through integration of denitrification activity within depth profiles (see *Laverman et al.* [2007] for similar calculations). Integration was performed using the trapezium rule, and the in situ denitrification rate in the 0–10 cm depth band was estimated by extrapolating the trend from measurements at 30, 20, and 10 cm data from shallow sediments to 0 cm depth.

#### 2.4.3. Damköhler Number Calculation

The Damköhler number for denitrification ($Da_N$) is the dimensionless ratio between a transport ($\tau_T$) and denitrification reaction ($\tau_R$) time scale. Parameter $\tau_T$ is the residence time (units = d), and $\tau_R$ is the inverse of the first-order reaction rate constant for denitrification, $K_1$ ($\tau_R = 1/K_1$, units for $K_1$ and $\tau_R$ are $d^{-1}$ and d, respectively) [*Harvey et al.*, 2013]. Our denitrification rates were zero order; i.e., production of $^{15}N$-labeled $N_2$ was linear with time. To convert our data to first-order rate constants we divided the zero-order rate constants (units = nmol $L^{-1}$ $h^{-1}$) by the mean half saturation constant for denitrification ($K_m$ = 109 μM) in rivers of north east England reported by *García-Ruiz et al.* [1998]. $Da_N$ ($\tau_T/\tau_R$) values $<1$ indicate that transport dominates over reaction, while values $>1$ indicate that reaction processes are occurring faster than advection [*Ocampo et al.*, 2006].

#### 2.4.4. Statistical Analysis

All statistics were performed in *R* [*R Development Core Team*, 2012]. Differences in chemical parameters across sediment depth bands and hydrologic settings were investigated by two-way analysis of variance (ANOVA). Prior to each ANOVA we tested whether the data were normally distributed with a Shapiro Wilk test and attempted to normalize any data where $p > 0.05$. For most variables, however, distributions were unable to be normalized using common methods (e.g., log and power transformations) so we rank transformed data prior to the ANOVA. Any significant effects detected in the ANOVA ($p > 0.05$) were further examined by pairwise comparisons using a Post-hoc Tukey's test. A paired $t$ test was used to test for any difference in the $^{15}N$ labeling of the $N_2$ and $N_2O$ pools following $^{15}NO_3^-$ addition. Relationships between denitrification rate and chemical variables were explored using Spearman's rank correlation.

## 3. Results

### 3.1. Summary of Reach Characteristics

#### 3.1.1. General Description of Stratigraphy

Median grain size ($d_{50}$) decreased with depth in the riverbed (Table 2); superficial sediments are a mixture of coarse sand, gravel, and small cobbles, while deep (>10 cm) sediments are mainly sand. Sediment particulate organic matter content was low, ranging from 0.3 to 3.3% (loss on ignition), and decayed with depth (ANOVA, $F(4,33) = 5.6$, $p = 0.002$).

#### 3.1.2. Spatial Distribution of Porewater Chemistry and Water Fluxes

Vertical head gradients were positive throughout the $^{15}N$ injections period (range = 0.5 to 28%) indicating upward movement of water from the sediments toward the river. Chloride profiles provided further evidence of porewater upwelling but also revealed localized zones of surface water downwelling and horizontal flows (e.g., plots B, F, and D, respectively; Figure 1c). We examined these water fluxes further using a two end-member mixing model, not to apportion water source in the riverbed, as depth profiles suggested at least three sources of water were present at some sites, but to quantitatively assign

**Table 2.** Median Solute Concentrations, Sediment Characteristics, and Vertical Water Flux by Depth in the Riverbed

| | Water (μM) | | | | Sediment | | | |
|---|---|---|---|---|---|---|---|---|
| Depth | $NO_3^-$ | DOC | $O_2$ | $Cl^-$ | LOI (%)[a] | $d_{50}$ (mm)[b] | Vertical Water flux (m $d^{-1}$) | *n*= |
| Surface | 125 | 187 | 276 | 701 | 0.9 | 6.5 | - | 7 |
| 10 cm | 128 | 170 | 142 | 433 | 1.1 | 2.2 | - | 15 |
| 20 cm | 240 | 166 | 149 | 408 | 0.8 | 0.62 | 0.12 | 14[c] |
| 30 cm | 227 | 139 | 180 | 418 | 0.5 | 0.42 | - | 14 |
| 50 cm | 200 | 143 | 157 | 410 | 0.5 | 0.44 | 0.02 | 14[c] |
| 100 cm | 303 | 165 | 197 | 409 | 0.4 | 0.37 | 0.04 | 15[c] |

[a]LOI denotes loss on ignition, a proxy measure of organic matter within sediment.
[b]$d_{50}$ represents median grain size.
[c]*n* for vertical flux measurements were 13, 14, and 14 for 20 cm, 50 cm, and 100 cm, respectively.

piezometer clusters to hydrologic settings. Subsurface hydrology could be described as either strong porewater upwelling, surface water downwelling to ≤20 cm (HEF), or horizontal flows ($n = 6$, 5, and 4, respectively; Figure 2). Water residence time, based on a calculated Darcy flux, varied from 0.11 d to 32 d for 10 cm and 50 cm flow pathways, respectively, when water flux was predominantly vertical (i.e., strong upwelling and/or HEF). Water residence times were slightly longer when upwelling was strong (mean ± SD = 5 ± 2 d and 3 ± 1 d for upwelling and HEF, respectively) and in deep sediments (mean ± SD = 0.7 ± 0.1 d and 2.2 ± 0.5 d/10 cm for sediments from 0 to 20 cm and 30–100 cm, respectively).

Porewater nitrate concentrations were highly variable, ranging from below detection to ≥600 μM at each of the depths examined. Overall, nitrate concentrations within deep sediments (100 cm) were higher than those in the river (mean ± SD = 311 ± 182 μM and 129 ± 18 μM, respectively) and tended to decrease toward the riverbed surface (Table 2). This trend was not statistically significant. Along-reach variation in porewater nitrate was also evident (Figure 3a), and concentrations were typically high in areas characterized by upwelling porewater (Figure 3b; $F(2,56) = 11.1$, $p < 0.001$).

Porewater DOC concentrations did not differ with depth in the riverbed (Table 2) relative to variation across the study reach (Figure 3c). Shallow sediments at 10 cm depth exposed to HEF were sites of elevated DOC (see points A, F, and H in Figure 3c and DOC concentrations summarized by depth and hydrology in the supporting information), although when integrating data across all depths (0–100 cm), differences between hydrologic settings were not significant (Figure 3d).

Porewaters were generally undersaturated in $O_2$ (mean ± SD = 49 ± 21%) and, like nitrate, oxygen concentrations decreased toward the riverbed surface (Table 2 and Figure 3e), although the trend was not

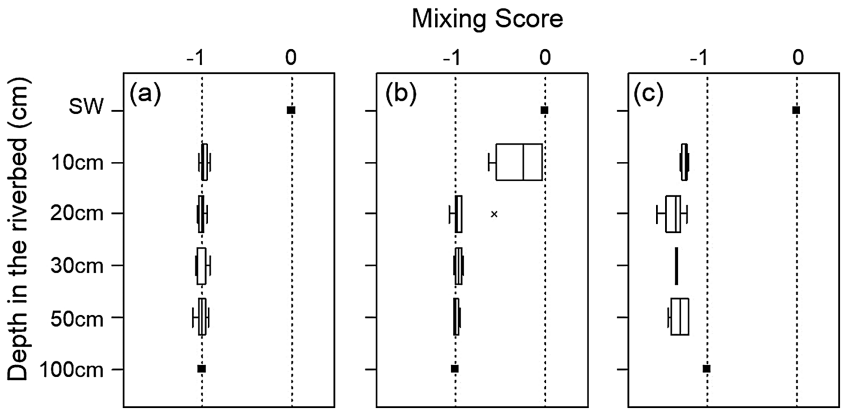


**Figure 2.** Characterization of subsurface hydrology using chloride concentrations in a mixing model. Mixing score is the output of a two end-member mixing model, modified such that porewater at 100 cm and surface water were equal to −1 and 0, respectively. The boxes consist of median values (straight vertical line), the interquartile range (limits of the box); whiskers are the minimum and maximum values; and outliers are plotted as crosses ($n = 6$, 5, and 4 per depth band, for (a) porewater upwelling, (b) hyporheic exchange flows (HEF), and (c) horizontal flows, respectively).

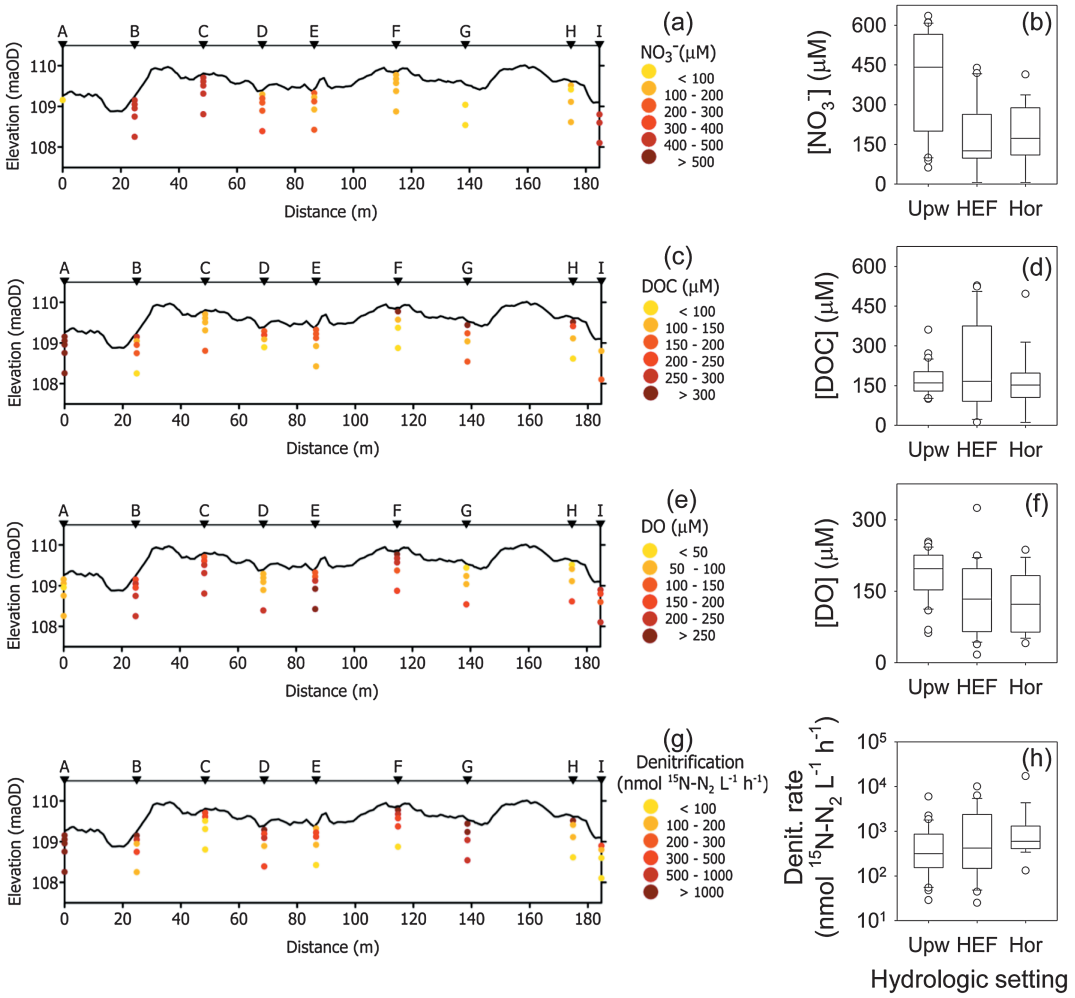


**Figure 3.** Spatial variation in porewater concentrations of (a and b) nitrate, (c and d) dissolved organic carbon, (e and f) dissolved oxygen, and (g and h) denitrification rate. Thalweg profiles (Figures 3a, 3c, 3e, and 3g) show individual data points from selected piezometers along the study reach (see Figure 1). Boxplots (Figures 3b, 3d, 3f, and 3h) contrast porewater chemistry and denitrification rate between hydrological settings with data from all piezometers. Boxes consist of median values (straight horizontal line), the interquartile range (limits of box), whiskers are the minimum and maximum values and outliers are plotted as circles.

statistically significant. When considering depth-distributions, dissolved oxygen concentrations were most heterogeneous at 10 cm depth in shallow sediments exposed to HEF (range = 308 μM, 17 to 325 μM). The next largest range in $O_2$ concentrations was 180 μM (57 to 237 μM) at 50 cm under horizontal water flux. Highest median $O_2$ concentrations were associated with sediments dominated by porewater upwelling (Figure 3f; ANOVA, $F(2,57) = 6.9$, $p = 0.002$), and these sediments were also associated with the lowest concentrations of other reduced chemical species such as Fe(II) and methane. Ammonium concentrations were highly variable both with depth in the riverbed and across the reach, ranging from below detection to 125 μM (mean ± SD = 5 ± 19 μM).

### 3.2. Factors Controlling In Situ Rates of Denitrification and Overall Nitrate Removal

#### 3.2.1. Quantification of In Situ Denitrification Rates

Rates of denitrification, as determined through the production of $^{15}N\text{-}N_2$, ranged from 25 to 17,053 nmol $^{15}N\,L^{-1}\,h^{-1}$, varying both with piezometer cluster and depth across the study reach (Figure 3g). We attribute this $^{15}N\text{-}N_2$ production to denitrification rather than anammox as the $^{15}N$-labeling of the $N_2$ and $N_2O$ pools were not significantly different ($t(49) = 0.766$, $p = 0.448$; Figure 4a and see below). The rate of denitrification generally decreased with depth in the riverbed (ANOVA, $F(4,57) = 4.0$, $p = 0.006$),

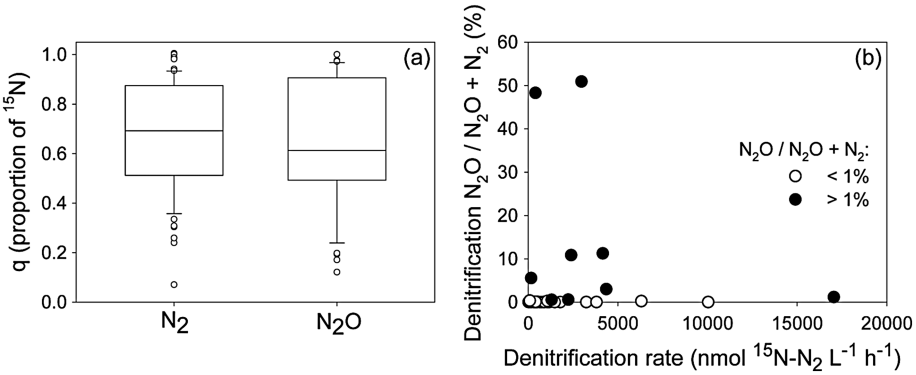


**Figure 4.** (a) Proportion of $^{15}N$ labeling in the $N_2$ and $N_2O$ pools and (b) proportion of $^{15}N$-labeled $N_2O$ in the total nitrogenous gas pool ($N_2 + N_2O$) produced from injection of $^{15}NO_3^-$ into the river bed ($n = 49$ per plot). Boxplots shown in Figure 4a consist of the median value (horizontal line), interquartile range (limits of the box), the minimum and maximum values (whiskers), and outliers are plotted as circles.

except where subsurface water flux was horizontal (Table 3). The relationship between depth and denitrification was strongest within sediments with upwelling porewater (Table 3) but overall, rates of denitrification here were lowest compared to sediments with HEF or horizontal flows ($F(2,57) = 3.6$, $p = 0.034$). In the presence of HEF, there was a clear "step down" between denitrification rates in shallow (<10 cm) and deep sediments (Table 3). Rates of denitrification increased with both the DOC concentration of porewater and organic matter content of sediment (as LOI; Table 4) and when porewater chemistry was reduced (i.e., low in $O_2$ and high Fe(II) and $CH_4$). We did, however, observe denitrification in seemingly oxygenated sediments (see the supporting information). Even when the porewater DO concentration was >200 μmol $L^{-1}$ $O_2$ (~60% of air saturation), denitrification could still be measured at up to 3249 nmol $^{15}N$-$N_2$ $L^{-1}$ $h^{-1}$ (median = 329 nmol $^{15}N$-$N_2$ $L^{-1}$ $h^{-1}$, $n = 21$)

In the majority of cases, denitrification was complete, i.e., $^{15}N$-$N_2$ comprised >99% of the $^{15}N$-labeled gas produced, but there were some samples where a considerable fraction of $^{15}NO_3^-$ reduction stopped at $N_2O$ (maximum $N_2O/N_2O + N_2 = 51\%$, median = 6%; $n = 9$ of the 49 examined). Although the patterns were not that strong, higher values for incomplete denitrification were most strongly correlated with high Fe(II) and $CH_4$, i.e., where sediments were most reduced.

The denitrification rates per unit volume were integrated over the top 100 cm to give an estimate of areal activity. Areal activity ranged from 132 to 4597 μmol $^{15}N$ $m^{-2}$ $h^{-1}$, with a median value of 480 μmol $^{15}N$ $m^{-2}$ $h^{-1}$ ($n = 15$). There was no significant difference between areal rates within different hydrological settings ($F(1,13) = 3.13$, $p = 0.01$; median areal rate = 479, 562 ,and 1026 μmol $^{15}N$ $m^{-2}$ $h^{-1}$ for strong upwelling, HEF, and horizontal fluxes, respectively).

### 3.2.2. Nitrate Export Using Damköhler Analysis

Controls on nitrate export were also investigated through calculation of Damköhler numbers, which varied both with depth and piezometer cluster across the study reach (range = 0.003 to 36, $n = 72$). The majority

**Table 3.** Rates of Denitrification Measured *In Situ* in the Riverbed

| | Denitrification (nmol $^{15}N$-$N_2$ $L^{-1}$ $h^{-1}$) | | | | |
|---|---|---|---|---|---|
| Depth | Range | Median[a] | Upwelling[b] | Hyporheic Exchange[b] | Horizontal[b] |
| 10 cm | 184–6314 | 1081 | 1075 | 1486 | 1062 |
| 20 cm | 148–10048 | 539 | 726 | 531 | 406 |
| 30 cm | 47–17053 | 362 | 257 | 246 | 644 |
| 50 cm | 29–4165 | 341 | 221 | 310 | 666 |
| 100 cm | 25–2977 | 178 | 132 | 78 | 509 |

[a] $n = 15$ for 10 and 100 cm depth bands and 14 for 20, 30, and 50cm depth bands.
[b] Data are median values, $n = 6$ for all upwelling depth bands, $n = 5$ for 10, 20, and 100 cm hyporheic exchange depth bands with $n = 4$ for the remaining depths in this setting, $n = 3$ for the 20 cm horizontal depth band with $n = 4$ for the remaining depths in this setting.

**Table 4.** Correlation between *In Situ* Rates of Denitrification (D15) and Chemical Composition of Porewater and Sediment[a]

| | D15 | $O_2$ | $NO_3^-$ | Fe(II) | $CH_4$ | DOC | LOI[b] |
|---|---|---|---|---|---|---|---|
| D15 | 1.00 | | | | | | |
| $O_2$ | −0.406** | 1.00 | | | | | |
| $NO_3^-$ | −0.362** | 0.547** | 1.00 | | | | |
| Fe(II) | 0.416** | −0.532** | −0.541** | 1.00 | | | |
| $CH_4$ | 0.394** | −0.269* | −0.442** | 0.566** | 1.00 | | |
| DOC | 0.357* | −0.219* | −0.126 | 0.509** | 0.297* | 1.00 | |
| LOI | 0.331* | −0.343* | −0.104 | −0.005 | 0.082 | 0.152 | 1.00 |

[a]Data are Spearman's rank correlation coefficients, $n = 72$ per test except.
[b]LOI where $n = 48$.
*$p < 0.05$.
**$p < 0.001$.

of values, however, were below the biogeochemical control threshold of $Da_N = 1$ (median = 0.14; Figure 5). $Da_N > 1$ ($n = 14$) were generally associated with deeper sediments (e.g., ≥20 cm) in two piezometer clusters, sites A and G, that were characterized by HEF and horizontal water fluxes, respectively.

### 3.2.3. Nitrate Attenuation in Riverbed Sediments

Deep sediments were important sites of nitrate attenuation, however, with ~80% of denitrification, on average, occurring between 10 and 100 cm depth in the riverbed (Table 5; depth-integrated data).

On a per centimeter basis, however, sediments within the 0–10 cm depth band were sites of enhanced nitrate removal under strong upwelling or HEF (Table 5; removal data per depth band divided by height of depth band). Total nitrate removal per piezometer cluster was highest in sites identified as biogeochemical hot spots (i.e., $Da_N > 1$, see above), similar when water flux was predominantly vertical (i.e., upwelling and HEF) and lowest when water flux was horizontal (Table 5). These differences, however, were not statistically significant.

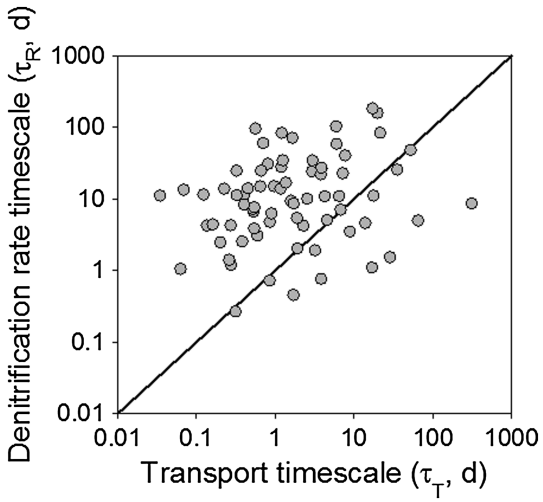


**Figure 5.** Time scales of denitrification versus time scales of water transport in a gaining reach (n=72). The solid line shows where the two time scales are equal, i.e., a Damköhler number of 1. Points that plot above the solid line represent sediments where water residence time is more important than denitrification rate in controlling nitrate flux ($Da_N < 1$). Points that plot above the solid line represent sediments where denitrification rate is the dominant controlling factor of nitrate flux ($Da_N > 1$).

## 4. Discussion

Here we have examined nitrate attenuation along upwelling flow pathways in a gaining reach low in organic carbon, measuring nitrogen transformations in situ, and simultaneously characterizing subsurface hydrology. Our integrated rates of denitrification (mean ± SE = 1078 ± 363 μmol $m^{-2}$ $h^{-1}$) are comparable to those measured by in situ "whole stream" $^{15}NO_3^-$ additions in rivers within agricultural catchments [*Mulholland et al.*, 2009]. Our work adds value to the existing evidence base of riverine nitrogen cycling because we also characterize denitrification below the zone of surface water-groundwater mixing. Denitrification occurred throughout the 100 cm depth of riverbed we examined, despite the limited amount of organic carbon and the moderate $O_2$ content of the upwelling porewater, demonstrating that the attenuation of nitrate is not just confined to shallow sediments within this groundwater-fed system. Our findings are consistent with those of *Storey et al.* [2004], *Fischer et al.* [2005], and *Stelzer et al.* [2011], and we show here that deep sediments are important sites of nitrate attenuation.

**Table 5.** Comparison of Nitrate Removal Calculated With and Without Inclusion of Water Residence Time in the Riverbed (Depth-Integrated and Rate-Determined, Respectively) and Across Different Hydrologic Settings

| Depth Band (cm) | Proportion of Nitrate Removal[a] | | Nitrate Removal (Depth-Integrated (mmol N $m^{-3}$)[b] | | | |
|---|---|---|---|---|---|---|
| | Rate-Determined | Depth-Integrated | Upwelling | Hyporheic Exchange | Horizontal | Hot Spots[c] |
| 0–10 | 0.36 | 0.19 | 2.7 | 7.0 | 1.2 | 24 |
| 10–20 | 0.28 | 0.12 | 1.8 | 1.1 | 0.5 | 45 |
| 20–30 | 0.16 | 0.05 | 1.8 | 0.9 | 1.1 | 24 |
| 30–50 | 0.12 | 0.25 | 3.5 | 4.2 | 3.8 | 486 |
| 50–100 | 0.08 | 0.39 | 6.1 | 2.5 | 5.0 | 687 |
| Median per cluster removal[d]: | | | 16 | 18 | 9 | 1259 |

[a]Data are average values, $n = 15$ per depth band.
[b]Data are median values within each hydrological setting and $n = 3$, 4, and 6 per depth band for horizontal fluxes, hyporheic exchange, and upwelling, respectively.
[c]Sites A and G are grouped as hot spots of denitrification (see text).
[d]Median per cluster removal is the median value of the sum of all depth bands, per piezometer cluster, i.e., median nitrate removal between 0 and 100 cm.

### 4.1. Pathways of Nitrate Reduction

Removal of nitrate along upwelling flow pathways could occur via a number of different metabolisms, e.g., denitrification, anammox, and assimilatory uptake [*Burgin and Hamilton*, 2007]. The fate of nitrate in the riverbed is important as the benefits of nitrate attenuation could be offset if the removal of nitrate occurs at the expense of production of more bioavailable and potentially harmful forms of nitrogen, e.g., $NH_4^+$ or $N_2O$ [*Burgin and Hamilton*, 2008; *Burgin et al.*, 2013]. In agreement with our previous slurry potential incubations [*Lansdown et al.*, 2012] there was no significant anammox activity in situ (proportion of $^{15}N$ in $N_2 = 0.57 \approx$ proportion of $^{15}N$ in $N_2O = 0.54$; Figure 4a) and all of the $^{15}N_2$ gas produced could be ascribed to denitrification. The decrease in the proportion of $^{15}N$ in $N_2$ or $N_2O$ relative to the injected $^{15}NO_3^-$ (98% $^{15}N$) tracer reflects mixing of the tracer plume with ambient porewater $^{14}NO_3^-$ pool.

For the majority of cases, denitrification was complete; however, for a subset of samples, a significant accumulation of $N_2O$ was measured (mean ± SD = 15 ± 20% $N_2O$, $n = 9$) peaking at 51%. Incomplete denitrification was not restricted to individual piezometer clusters, particular hydrologic settings or sediment depths. The production of $N_2O$ in soils is well characterized but it is poorly constrained in rivers, although the data available suggest a strong influence of hypoxia [*Rosamond et al.*, 2012] and here most of the variance in the accumulation of $N_2O$ was correlated with patches of low redox environment (accumulated $NH_4^+$, Fe(II), and methane) and enhanced microbial activity (low $O_2$ saturation and fast rates of denitrification). Given that $N_2O$ has a greenhouse warming potential ~280 times than that of $CO_2$ [*Reay et al.*, 2012], the potential environmental trade-off between nitrate attenuation and potent greenhouse gas production via riverbed denitrification warrants further investigation.

### 4.2. Interplay Between Hydrological and Biogeochemical Controls

#### 4.2.1. The Role of HEFs in Controlling In Situ Denitrification

*Stelzer and Bartsch* [2012] described a conceptual model whereby nitrate removal within gaining reaches receiving oxygenated groundwater will proceed only when the upwelling flow path interacts with favorable redox conditions created through degradation of deposited and buried particulate organic matter. A similar explanation was given for patterns in nitrate concentrations in the River Tern, except that clay or peat lenses rather than particulate organic carbon derived from ingression, controlled nitrate removal [*Krause et al.*, 2013]. Here we have quantified denitrification activity to 100 cm depth in a riverbed that comprised <1% organic matter, on average (maximum LOI = 3%, cf. average ~12 %, maximum = 50 % in *Stelzer and Bartsch* [2012]. We found no evidence for lenses of buried organic matter up-gradient of the flow pathways in this reach despite extensive drilling within the study site (>100 piezometers within a 200 m reach).

It would appear that nitrate removal within this gaining reach does not require meter-scale patches of buried particulate organic matter to generate favorable redox conditions for denitrification to occur (in the sense of *Krause et al.* [2013]). Rather, we propose that inputs of DOC and particulate organic carbon to the riverbed (i)

from HEF (in the sense of *Stelzer and Bartsch* [2012]) and (ii) via subsurface routes from the floodplain or riparian zone are the key mechanisms driving heterotrophic denitrification in this instance. Conceptually, HEFs could either stimulate denitrification activity by supply of labile organic carbon to the sediments or suppress denitrification activity as well-oxygenated surface water downwells. Here as with our previous centimeter-scale investigation [*Lansdown et al.*, 2014], denitrification was observed in porewaters with $O_2$ concentrations $>200\,\mu M$, although this activity is probably confined to anoxic microsites within oxygenated sediments [*Triska et al.*, 1993]. The role that HEFs play in increasing nitrate attenuation capacity of riverbeds (as per *Fischer et al.* [2005], *Harvey et al.* [2013], and *Zarnetske et al.* [2011]) can be observed in our shallow sediments ($<10$ cm depth; Table 3) around piezometer clusters A, C2 (right margin), F, H, and I. In these sediments, dissolved $O_2$ concentrations were elevated, approaching air-equilibrated values in some cases, indicating ingress of well-oxygenated surface water (i.e., HEFs). Supply of organic matter from the river above through HEFs is inferred from elevated concentrations of DOC in porewaters at 10 cm, as well as accumulation of products of mineralization (ammonium and methane; see supporting information). Here 44% of total depth-integrated nitrate removal (0–100 cm depth) occurred within 10 cm of the sediment surface highlighting the increased denitrification capacity of sediments under HEFs.

It is, however, more difficult to account for the increased denitrification activity in shallow sediments where strong porewater upwelling suppresses groundwater-surface water exchange (as seen in chloride depth profiles of piezometer clusters B, C, and D; Figure 1c). Within this hydrological setting approximately 17% of total depth-integrated nitrate removal (0–100 cm depth) occurred in the top 10 cm of the riverbed. Here we aimed to characterize riverbed nitrate removal under base flow conditions. A parallel study at this site has quantified the effect of rising river stage on porewater chemistry, finding that stage increase can cause reversal in the vertical hydraulic gradient, potentially allowing surface water to infiltrate areas of the riverbed where no exchange occurs under low flow conditions, altering porewater chemistry [*Byrne et al.*, 2013]. Our finding of enhanced nitrate attenuation capacity within shallow sediments, with little apparent hydrological connection to surface water, or the floodplain, could be explained by groundwater-surface water exchange or horizontal inputs under high flows (e.g., storm events) prior to the sampling campaign. The potential for such event flows to alter biogeochemical cycling, and the time scale over which processes could be affected, is poorly understood in rivers [*Zimmer and Lautz*, 2014]. Through a combination of modeling and laboratory simulation, *Gu et al.* [2008] have shown that nitrate attenuation, via denitrification in upwelling groundwater, can be altered simply through changes in residence times caused by hydraulic head variation associated with river stage rise. They did not explicitly consider what biogeochemical effects stage variation could have on the subsurface chemistry, but if a change in river stage can alter nitrate attenuation by altering residence times, even after the "event flow" has passed [*Gu et al.*, 2008], porewater chemistry and associated biogeochemical cycling (i.e., rates of denitrification) could be similarly affected.

#### 4.2.2. Are Hot Spots of Denitrification Related to Horizontal Flow Pathways?

Variation in the direction and magnitude of water fluxes alter both residence time and subsurface chemistry within the riverbed, thus affecting not only the depth distribution of biogeochemical activity, but also spatial zonation of processes such as denitrification across the riverbed. At sites A and G, the total depth-integrated rate of denitrification was 2 orders of magnitude higher than the rest of the reach (1259 mmol N $m^{-3}$). Here porewaters were very reduced (low $O_2$ and high ammonium and methane), denitrification rates were very high and Damköhler numbers were $>1$, indicating that nitrate export is controlled by reaction rate rather than residence time. These sites were previously identified as biogeochemical hot spots by *Heppell et al.* [2013], where horizontal water fluxes (defined as lateral inputs or HEFs) dominated over groundwater upwelling, supplying organic matter to the subsurface which was then mineralized. *Heppell et al.* [2013] suggested that these sites would exhibit enhanced nitrate removal, and for these patches of riverbed this is indeed the case. From more spatially extensive porewater chemistry obtained through previous work [*Heppell et al.*, 2013; *Lansdown et al.*, 2014] we estimate that such biogeochemical hot spots cover approximately 2.5% of the study reach (~47 $m^2$) but, within which, 8% of the nitrate removal within the top 1 m of riverbed occurs (average removal within these biogeochemical hot spots divided by average removal across the rest of the reach). These estimates of nitrate removal along horizontal flow pathways were performed assuming a maximum flow path of 1 m. Where flow pathways were horizontal, rather

than vertical, we assume that vertical and horizontal water fluxes were equal, on average [see *Binley et al.*, 2013] and therefore that the flow pathway is approximately 45°. As such, there will be no net effect on residence time over the flow pathway if the direction of flow is horizontal rather than vertical. However, this research also shows that not every area characterized by horizontal flows is a hot spot of nitrate reduction. In fact, for three out of the four zones associated with horizontal water movement, there was less nitrate removed from the top 100 cm of sediments compared to the vertical flow settings (9 mmol N $m^{-3}$). The reasons for this warrant further research but it is likely that variation in the origin and length of horizontal flow paths across the reach will influence the quality of the DOC; for example, some horizontal pathways will originate from the nearby riparian and floodplain areas potentially comprising labile DOC while others will be from deeper groundwater and potentially be characterized by more recalcitrant DOC compounds.

Through geophysical measurements *Binley et al.* [2013] also identified a preferential discharge zone in this reach at sites B to D, where upwelling porewater flux was very strong and, as a result, there was little exchange with surface water or horizontal water inputs. The short water residence time, combined with the high nitrate load in the oxygenated upwelling porewater, led *Heppell et al.* [2013] to propose that nitrate removal would be minimal within this patch of the riverbed. Our results also support this finding as this preferential discharge zone is indeed a cold spot for denitrification: occupying ~20% of the reach area [*Binley et al.*, 2013] but performing <2% of the total denitrification that occurs within the reach (average removal from sites B, C, and D divided by average removal across the rest of the reach).

#### 4.2.3. The Importance of Deep Sediments for Nitrate Attenuation

Across the reach as a whole, denitrification within the top 1 m of the riverbed removed between 0.3 and 32% of nitrate exported from upwelling porewater (median = 9%) but denitrification activity was not equally distributed with depth or hydrologic setting. Considering rates of denitrification alone (see rate-determined denitrification in Table 5), as per *Stelzer et al.* [2011], deep sediments (>10 cm) accounted for 64% of subsurface nitrate removal. However, simply integrating denitrification rates over a given depth to estimate overall nitrate removal within a volume of sediments ignores the potential influence of water residence time on nitrate flux, which can be an important predictor of the fate of nitrate in sediments [*Zarnetske et al.*, 2011]. Damköhler numbers indicate that riverbed nitrate attenuation within this gaining reach is limited by the rate of denitrification (i.e., $Da_N < 1$; Figure 5) and, as a result, nitrate flux to the river above is more strongly controlled by water residence time. When nitrate attenuation is considered as the interaction of hydrology and biogeochemistry (i.e., the product of denitrification rate and water residence time) we calculate that, on average, 81% of subsurface nitrate removal occurred within deep sediments (depth-integrated denitrification in Table 5). Nitrate removal of the magnitude presented in Table 5 could only occur if the supply of nitrate in the upwelling porewater exceeded the removal capacity of the sediments. Measured porewater nitrate concentrations compare favorably with those predicted from depth-integrated nitrate loss except in the sites identified as biogeochemical hot spots (Figure S2 in the supporting information), suggesting that data presented in Table 5 are likely indicative of actual rather than potential nitrate removal in the sediments.

Maximum nitrate removal will occur when time scales of denitrification and water residence time are well matched [*Gu et al.*, 2007], but nitrate attenuation can also be enhanced when denitrification rate is fast but water residence time is short, or vice versa. *Harvey et al.* [2013] explained equal contributions of fine marginal and coarse thalweg sediments to hyporheic nitrate removal via this mechanism. Here we show that such a relationship can also explain nitrate removal with depth in a gaining reach. Where groundwater flux was predominantly vertical (i.e., strong upwelling or HEF), denitrification rates decayed with depth as the influence of the river on the sediments below diminished (see above). Saturated hydraulic conductivity and vertical hydraulic gradients were lower in deep sediments (50 cm and 100 cm [*Binley et al.*, 2013]) resulting in longer water residence times. Consequently, shallow sediments (10 cm and 20 cm) were characterized by fast denitrification but short residence time, while in deep sediment denitrification was slow and residence time was long, with a switch between the two scenarios at ~30 cm (Figure 6). These results illustrate that both physical and biogeochemical controls on nitrate attenuation, and the interaction thereof, can vary along upwelling flow pathways in a gaining reach.

Prior use of Damköhler numbers to investigate nitrate flux within streambeds and the riparian zone has assumed denitrification rate and/or water flux to be constant along flow pathways [*Gu et al.*, 2007; *Ocampo et al.*, 2006]. Both our study and that of *Harvey et al.* [2013] highlight the variability of

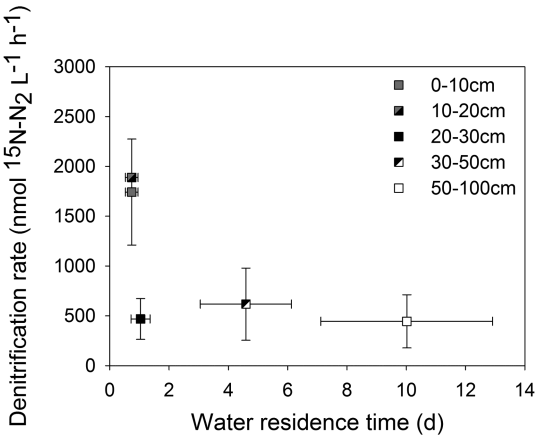


**Figure 6.** Variation of denitrification rate and water residence time with depth in the bed of gaining river, showing an interchange between the importance of factors controlling nitrate removal between shallow and deep sediments. Data are average values with error bars of 1 standard deviation.

denitrification and water flux time scales across relatively small spatial scales (e.g., m to dm). Here we have shown in a gaining reach that denitrification is most variable within shallow sediments, while high variation in water residence time is associated with deep sediments and therefore use of a single denitrification rate and water flux value to categorize nitrate transport is simply not appropriate.

## 5. Conclusion

The results of this study provide quantitative evidence for nitrate attenuation within the bed of a groundwater-fed river that is controlled by both biogeochemical and hydrologic processes. We have shown that denitrification occurs within carbon-poor, sandy sediments to a depth of at least 1 m below the riverbed surface without substantial deposits of buried organic matter, at rates that are generally low, but a similar order of magnitude to the global evidence base of rivers in agricultural landscapes. The majority of nitrate attenuation in our reach is transport-controlled irrespective of the flow pathway (vertical or horizontal). In the case of the River Leith, hyporheic exchange flows and horizontal water fluxes such as shallow groundwater inputs from the floodplain or riparian zone are important because they supply the precursor substrates needed to sustain denitrification. We identified two hot spots of denitrification (which are reaction rate controlled) located within areas of hyporheic exchange or horizontal water flux, and we estimate that these zones account for 8% of overall nitrate attenuation in the bed sediments.

Both reaction rate and water residence times change with depth in the riverbed under stable, low flow conditions. Along an upwelling flow pathway residence time is the most important control on nitrate removal at depth (>20 cm) while the rate of denitrification increases and leads to enhanced nitrate removal near the sediment surface. Overall, our results highlight the importance of using measurements of both biogeochemical reaction rates and residence time to estimate the extent of nitrate removal from riverbed sediments because, in our reach, ignoring residence time underestimates the importance of deep sediments for nitrate removal by about 20%.

We recommend that future work should not only continue to explore factors controlling variation in transport and rate-limited reactions at the reach scale, but also to attempt to upscale such analysis to consider the effect of different hydrogeological settings on the balance of biogeochemical and hydrological controls influencing nitrate removal.

**Acknowledgments**

This work was funded by a Natural Environment Research Council grant awarded to Lancaster University (NE/F006063/1) and Queen Mary University of London NE/F004753/1 and NE/J012106/1. We acknowledge the Eden Rivers Trust and Lowther Estates in facilitating access to the site, the Environment Agency (England and Wales) in giving consent to establishing the experimental setup in the river, and Lancaster University for installing and maintaining the physical hydrology instrumentation in the river. We thank two anonymous reviewers for their comments which helped strengthen this paper. The data presented are available upon request from the corresponding author.

## References

Addy, K., D. Q. Kellogg, A. J. Gold, P. M. Groffman, G. Ferendo, and C. Sawyer (2002), In situ push-pull method to determine ground water denitrification in riparian zones, *J. Environ. Qual.*, *31*(3), 1017–1024, doi:10.2134/jeq2002.1017.

Allen, D. J., J. P. Bloomfield, and V. K. Robinson (1997), The physical properties of major aquifers in England and Wales, British Geological Survey Tech. Rep. WD/97/34. 312 pp., Natural Environment Research Council and Environment Agency.

APHA-AWWA-WPCF (1976), *Standard Methods for the Examination of Water and Wastewater*, pp. 208, American Public Health Association, Washington, D. C.

Bahr, J. M., and J. Rubin (1987), Direct comparison of kinetic and local equilibrium formulations for solute transport affected by surface reactions, *Water Resour. Res.*, *23*(3), 438–452, doi:10.1029/WR023i003p00438.

Bardini, L., F. Boano, M. B. Cardenas, R. Revelli, and L. Ridolfi (2012), Nutrient cycling in bedform induced hyporheic zones, *Geochim. Cosmochim. Acta*, *84*, 47–61, doi:10.1016/j.gca.2012.01.025.

Bernot, M. L., and W. K. Dodds (2005), Nitrogen retention, removal, and saturation in lotic ecosystems, *Ecosystems*, *8*, 442–453.

Binley, A., S. Ullah, A. L. Heathwaite, C. Heppell, P. Byrne, K. Lansdown, M. Trimmer, and H. Zhang (2013), Revealing the spatial variability of water fluxes at the groundwater-surface water interface, *Water Resour. Res.*, *49*, 3978–3992, doi:10.1002/wrcr.20214.

Burgin, A. J., and S. K. Hamilton (2007), Have we overemphasized the role of denitrification in aquatic ecosystems? A review of nitrate removal pathways, *Front. Ecol. Environ.*, *5*(2), 89–96, doi:10.1890/1540-9295(2007)5[89:HWOTRO]2.0.CO;2.

Burgin, A. J., and S. K. Hamilton (2008), $NO_3^-$ - driven $SO_4^{2-}$ production in freshwater ecosystems: Implications for N and S cycling, *Ecosystems*, *11*, 908–922.
Burgin, A. J., J. G. Lazar, P. M. Groffman, A. J. Gold, and D. Q. Kellogg (2013), Balancing nitrogen retention ecosystem services and greenhouse gas disservices at the landscape scale, *Ecol. Eng.*, *56*, 26–35, doi:10.1016/j.ecoleng.2012.05.003.
Burt, T. P., N. J. K. Howden, F. Worrall, M. J. Whelan, and M. Bieroza (2011), Nitrate in United Kingdom rivers: Policy and its outcomes since 1970, *Environ. Sci. Technol.*, *45*(1), 175–181, doi:10.1021/es101395s.
Byrne, P., A. Binley, A. L. Heathwaite, S. Ullah, C. M. Heppell, K. Lansdown, H. Zhang, M. Trimmer, and P. Keenan (2013), Control of river stage on the reactive chemistry of the hyporheic zone, *Hydrol. Process.*, *28*(17), 4766–4779, doi:10.1002/hyp.9981.
Caraco, N. F., and J. J. Cole (1999), Human impact on nitrate export: An analysis using major world rivers, *Ambio*, *28*(2), 167–170.
Clilverd, H., J. Jones Jr., and K. Kielland (2008), Nitrogen retention in the hyporheic zone of a glacial river in interior Alaska, *Biogeochemistry*, *88*(1), 31–46, doi:10.1007/s10533-008-9192-9.
Findlay, S. E. G., R. L. Sinsabough, W. V. Sobczak, and M. Hoostal (2003), Metabolic and structural response of hyporheic microbial communities to variations in supply of dissolved organic matter, *Limnol. Oceanogr.*, *48*(4), 1608–1617.
Fischer, H., F. Kloep, S. Wilzcek, and M. T. Pusch (2005), A river's liver - microbial processes within the hyporheic zone of a large lowland river, *Biogeochemistry*, *76*(2), 349–371, doi:10.1007/s10533-005-6896-y.
García-Ruiz, R., S. N. Pattinson, and B. A. Whitton (1998), Kinetic parameters of denitrification in a river continuum, *Appl. Environ. Microbiol.*, *64*(7), 2533–2538.
Grace, M. R., T. R. Scicluna, C. L. Vithana, P. Symes, and K. P. Lansdown (2010), Biogeochemistry and cyanobacterial blooms: investigating the relationship in a shallow, polymictic, temperate lake, *Environ. Chem.*, *7*, 443–456, doi:10.1071/EN10042.
Gu, C., G. M. Hornberger, A. L. Mills, J. S. Herman, and S. A. Flewelling (2007), Nitrate reduction in streambed sediments: Effects of flow and biogeochemical kinetics, *Water Resour. Res.*, *43*(12), W12413, doi:10.1029/2007WR006027.
Gu, C., G. M. Hornberger, J. S. Herman, and A. L. Mills (2008), Effect of freshets on the flux of groundwater nitrate through streambed sediments, *Water Resour. Res.*, *44*, W05415, doi:10.1029/2007WR006488.
Harvey, J. W., J. K. Böhlke, M. A. Voytek, D. Scott, and C. R. Tobias (2013), Hyporheic zone denitrification: Controls on effective reaction depth and contribution to whole-stream mass balance, *Water Resour. Res.*, *49*, 6298–6316, doi:10.1002/wrcr.20492.
Heppell, C., A. Louise Heathwaite, A. Binley, P. Byrne, S. Ullah, K. Lansdown, P. Keenan, M. Trimmer, and H. Zhang (2013), Interpreting spatial patterns in redox and coupled water–nitrogen fluxes in the streambed of a gaining river reach, *Biogeochemistry*, *117*(2–3), 491–509, doi:10.1007/s10533-013-9895-4.
Howden, N. J. K., and T. P. Burt (2008), Temporal and spatial analysis of nitrate concentrations from the Frome and Piddle catchments in Dorset (UK) for water years 1978 to 2007: Evidence for nitrate breakthrough?, *Sci. Total Environ.*, *407*(1), 507–526, doi:10.1016/j.scitotenv.2008.08.042.
Istok, J. D., M. D. Humphrey, M. H. Schroth, M. R. Hyman, and K. T. O'Reilly (1997), Single-well, "push-pull" test for *in situ* determination of microbial activities, *Ground Water*, *35*(4), 619–631.
Knapp, M. F. (2005), Diffuse pollution threats to groundwater: A UK water company perspective, *Q. J. Eng. Geol. Hydrogeol.*, *38*(1), 39–51, doi:10.1144/1470-9236/04-015.
Krause, S., C. Tecklenburg, M. Munz, and E. Naden (2013), Streambed nitrogen cycling beyond the hyporheic zone: Flow controls on horizontal patterns and depth distribution of nitrate and dissolved oxygen in the upwelling groundwater of a lowland river, *J. Geophys. Res. Biogeosci.*, *118*, 54–67, doi:10.1029/2012JG002122.
Lansdown, K., M. Trimmer, C. M. Heppell, F. Sgouridis, S. Ullah, A. L. Heathwaite, A. Binley, and H. Zhang (2012), Characterization of the key pathways of dissimilatory nitrate reduction and their response to complex organic substrates in hyporheic sediments, *Limnol. Oceanogr.*, *57*(2), 387–400, doi:10.4319/lo.2012.57.2.0387.
Lansdown, K., C. M. Heppell, M. Dossena, S. Ullah, A. L. Heathwaite, A. Binley, H. Zhang, and M. Trimmer (2014), Fine-scale *in situ* measurement of riverbed nitrate production and consumption in an armored permeable riverbed, *Environ. Sci. Technol.*, *48*(8), 4425–4434, doi:10.1021/es4056005.
Lapworth, D. J., D. C. Gooddy, A. S. Butcher, and B. L. Morris (2008), Tracing groundwater flow and sources of organic carbon in sandstone aquifers using fluorescence properties of dissolved organic matter (DOM), *Appl. Geochem.*, *23*(12), 3384–3390, doi:10.1016/j.apgeochem.2008.07.011.
Laverman, A. M., C. Meile, P. Van Cappellen, and E. B. A. Wieringa (2007), Vertical distribution of denitrification in an estuarine sediment: Integrating sediment flowthrough reactor experiments and microprofiling via reactive transport modeling, *Appl. Environ. Microbiol.*, *73*(1), 40–47, doi:10.1128/aem.01442-06.
Maier, G., R. J. Nimmo-Smith, G. A. Glegg, A. D. Tappin, and P. J. Worsfold (2009), Estuarine eutrophication in the UK: current incidence and future trends, *Aquat. Conserv.*, *19*(1), 43–56, doi:10.1002/aqc.982.
Marzadri, A., D. Tonina, and A. Bellin (2011), A semianalytical three-dimensional process-based model for hyporheic nitrogen dynamics in gravel bed rivers, *Water Resour. Res.*, *47*, W11518, doi:10.1029/2011WR010583.
Mulholland, P. J., et al. (2009), Nitrate removal in stream ecosystems measured by N-15 addition experiments: Denitrification, *Limnol. Oceanogr.*, *54*(3), 666–680, doi:10.4319/lo.2009.54.3.0666.
Nielsen, L. P. (1992), Denitrification in sediment determined from nitrogen isotope pairing, *FEMS Microbiol. Ecol.*, *86*, 357–362.
Ocampo, C. J., C. E. Oldham, and M. Sivapalan (2006), Nitrate attenuation in agricultural catchments: Shifting balances between transport and reaction, *Water Resour. Res.*, *42*(1), W01408, doi:10.1029/2004WR003773.
Office, N. A. (2010), Tackling diffuse water pollution in England, Report by the Comptroller and Auditor General, Report No. HC 188 Session 2010–2011, London.
R Development Core Team (2012), R: A language and environment for statistical computing, R Foundation for Statistical Computing, Vienna, Austria.
Reay, D. S., E. A. Davidson, K. A. Smith, P. Smith, J. M. Melillo, F. Dentener, and P. J. Crutzen (2012), Global agriculture and nitrous oxide emissions, *Nat. Clim. Change*, *2*(6), 410–416, doi:10.1038/nclimate1458.
Risgaard-Petersen, N., L. P. Nielsen, S. Rysgaard, T. Dalsgaard, and R. L. Meyer (2003), Application of the isotope pairing technique in sediments where anammox and denitrification coexist, *Limnol. Oceanogr. Methods*, *1*, 63–73.
Rivett, M. O., S. R. Buss, P. Morgan, J. W. N. Smith, and C. D. Bemment (2008), Nitrate attenuation in groundwater: A review of biogeochemical controlling processes, *Water Res.*, *42*, 4215–4232, doi:10.1016/j.watres.2008.07.020.
Rosamond, M. S., S. J. Thuss, and S. L. Schiff (2012), Dependence of riverine nitrous oxide emissions on dissolved oxygen levels, *Nat. Geosci.*, *5*(10), 715–718, doi:10.1038/ngeo1556.
Sanders, I. A., and M. Trimmer (2006), *In situ* application of the $^{15}NO_3^-$ isotope pairing technique to measure denitrification in sediments at the surface water–groundwater interface, *Limnol. Oceanogr. Methods*, *4*, 142–152.

Seymour, K., J. Atkins, A. Handoo, P. Hulme, and K. Wilson (2008), *Investigation into groundwater-surface water interactions and the hydro-ecological implications of two groundwater abstractions in the River Leith catchment, a sandstone system in the Eden Valley, Cumbria*, U. K. Environment Agency, Warrington.

Sheibley, R. W., J. H. Duff, A. P. Jackman, and F. J. Triska (2003), Inorganic nitrogen transformations in the bed of the Shingobee River, Minnesota: Integrating hydrologic and biological processes using sediment perfusion cores, *Limnol. Oceanogr.*, *48*(3), 1129–1140, doi:10.4319/lo.2003.48.3.1129.

Smart, R. M., and J. W. Barko (1985), Laboratory culture of submersed freshwater macrophytes on natural sediments, *Aquat.Bot.*, *21*, 251–263, doi:10.1016/0304-3770(85)90053-1.

Smith, J. W. N. (2005), Groundwater-surface water interactions in the hyporheic zone, Environment Agency (UK) Science Report, Report No. SC030155/SR1.

Smith, J. W. N., and D. N. Lerner (2008), Geomorphologic control on pollutant retardation at the groundwater–surface water interface, *Hydrol. Processes*, *22*(24), 4679–4694, doi:10.1002/hyp.7078.

Stelzer, R. S., and L. A. Bartsch (2012), Nitrate removal in deep sediments of a nitrogen-rich river network: A test of a conceptual model, *J. Geophys. Res.*, *117*, G02027, doi:10.1029/2012JG001990.

Stelzer, R. S., L. A. Bartsch, W. B. Richardson, and E. A. Strauss (2011), The dark side of the hyporheic zone: Depth profiles of nitrogen and its processing in stream sediments, *Freshwater Biol.*, *56*(10), 2021–2033, doi:10.1111/j.1365-2427.2011.02632.x.

Storey, R. G., D. D. Williams, and R. R. Fulthorpe (2004), Nitrogen processing in the hyporheic zone of a pastoral stream, *Biogeochemistry*, *69*(3), 285–313, doi:10.1023/B:BIOG.0000031049.95805.ec.

Thamdrup, B., and T. Dalsgaard (2000), The fate of ammonium in anoxic manganese oxide-rich marine sediment, *Geochim. Cosmochim. Acta*, *64*(24), 4157–4164, doi:10.1016/S0016-7037(00)00496-8.

Trimmer, M., N. Risgaard-Petersen, J. C. Nicholls, and P. Engström (2006), Direct measurement of anaerobic ammonium oxidation (anammox) and denitrification in intact sediment cores, *Mar. Ecol. Prog. Ser.*, *326*, 37–47, doi:10.3354/meps326037.

Triska, F. J., J. H. Duff, and R. J. Avanzino (1993), The role of water exchange between a stream channel and its hyporheic zone in nitrogen cycling at the terrestrial aquatic interface, *Hydrobiologia*, *251*(1–3), 167–184, doi:10.1007/BF00007177.

Zarnetske, J. P., R. Haggerty, S. Wondzell, and M. A. Baker (2011), Dynamics of nitrate production and removal as a function of residence time in the hyporheic zone, *J. Geophys. Res.*, *116*, G01025, doi:10.1029/2010JG001356.

Zarnetske, J. P., R. Haggerty, S. M. Wondzell, V. A. Bokil, and R. González-Pinzón (2012), Coupled transport and reaction kinetics control the nitrate source-sink function of hyporheic zones, *Water Resour. Res.*, *48*(11), W11508, doi:10.1029/2012WR011894.

Zimmer, M. A., and L. K. Lautz (2014), Temporal and spatial response of hyporheic zone geochemistry to a storm event, *Hydrol. Process.*, *28*(4), 2324–2337, doi:10.1002/hyp.9778.